

Exact non-Hookean scaling of cylindrically bent elastic sheets and the large-amplitude pendulum

Vyacheslavas Kashcheyevs^{a)}

Faculty of Physics and Mathematics, University of Latvia, Zellu Street 8, Riga LV-1002, Latvia

(Received 26 August 2010; accepted 7 January 2011)

A sheet of elastic foil rolled into a cylinder and deformed between two parallel plates acts as a non-Hookean spring if deformed normally to the axis. For large deformations the elastic force shows an interesting inverse square dependence on the interplate distance. This phenomenon was used as the basis for an experimental problem at the 41st International Physics Olympiad. We show that the corresponding variational problem for the equilibrium energy of the deformed cylinder is equivalent to a minimum action description of a simple gravitational pendulum with an amplitude of 90° . We use this analogy to show that the power-law of the force is exact for distances less than a critical value. An analytical solution for the elastic force is found and confirmed by measurements over a range of deformations covering both linear and nonlinear behaviors. © 2011 American Association of Physics Teachers.

[DOI: 10.1119/1.3553232]

I. INTRODUCTION

Šiber and Buljan analyzed the following simple yet pedagogically rich problem from the theory of elasticity.¹ A thin flat elastic sheet (for example, a piece of plastic foil) is rolled into a cylinder of radius b_0 and placed between two impenetrable parallel plates which are parallel to the axis of the cylinder, as shown in Fig. 1. The distance $2b$ between the plates is fixed externally. For $b < b_0$ the foil acts as a spring and exerts a force of magnitude $F(b)$ on each of the plates. An interesting property of this spring is the nonlinear power-law dependence of the elastic force, $F \propto b^{-2}$, which we will show is exact for $b < b_c \approx 0.7b_0$. Measuring $F(b)$ for $b < b_c$ has been proposed as a way to determine the bending rigidity of objects such as plastic foils, electrical connectors, biological membranes and microtubules, and possibly nanotubes and monolayer materials (for example, graphene).¹

A laboratory problem based on measuring $F(b)$ for plastic transparency films was recently given to the world's top secondary school physics students at the 41st International Physics Olympiad (Zagreb, Croatia, 2010). The corresponding theoretical problem of constrained minimization of the foil's elastic energy might seem difficult. The solution¹ is based on analytical approximations and finite element optimization, and a textbook approach² relies on force equilibrium conditions for strongly bent elastic rods that are rarely covered in standard physics curricula.

In this paper, we formulate and solve the variational problem for the minimal energy of deformed elastic cylinder using tangential angle parametrization of the profile shape. The solution reveals an equivalence to another conceptually rich physics system—the large-amplitude pendulum. We will see that the elastic energy of the foil maps onto the kinetic energy of the pendulum, and the fixed interplate distance maps onto the cosine-shape potential energy of the pendulum. Simple mechanical considerations allow us to deduce the exact inverse square dependence for the elastic force for $b < b_c$. By using the standard solution for the large-amplitude pendulum in terms of elliptic functions, we find the exact values for b_c and related constants, a single transcendental equation that determines $F(b)$ for $b > b_c$, and a compact analytic form for the profile of the deformed cylinder. The func-

tional dependence of $F(b)$ is compared to measurements on a plastic film in the table-top setup used in Ref. 1. Thus, it is feasible to obtain a quantitative demonstration of both the nonlinear law force law for $b < b_c$ and the usual linear regime for $b \rightarrow b_0$.

II. FORMULATION OF THE PROBLEM

A property of the deformation geometry in this problem is that the Gaussian curvature vanishes at every point. This property eliminates nonuniform stretching/compression (see Ref. 2, Sec. 14) and leaves only the bending contribution to the total elastic energy W for thin sheets (thickness $d \ll b_0$). The problem is essentially one-dimensional and the energy functional is the same as for an elastic filament (a Kirchhoff rod, see Ref. 2, Sec. 18), and is given by

$$W = \frac{\kappa h}{2} \int K[x(s), y(s)]^2 ds, \quad (1)$$

where the effects of gravity are ignored. Here $\kappa = (1 - \nu^2)^{-1} E d^3 / 12$ is the bending rigidity, E is the bulk Young modulus of the foil, ν is the Poisson ratio, h is the length of the cylinder in the nondeformed direction (that is, parallel to the axis), and K is the planar curvature of the deformation profile in the plane normal to the axis (the x - y plane). The shape of the profile is described using the natural parametrization³ $\{x(s), y(s)\}$ in the coordinate system defined in Fig. 2(a) with the origin at point O , and s is the arc length measured counterclockwise from O .

The integration in Eq. (1) is performed along the entire profile, and the absence of stretching⁴ implies that $\int ds = 2\pi b_0$ regardless of b . The constraint imposed by the plates is expressed by requiring that the vertical coordinate of point O' is $2b$ [see Fig. 2(a)],

$$x(s = \pi b_0) = 2b. \quad (2)$$

In the following, we find the minimum of W subject to the constraint (2) and the impenetrability of the plates. The elastic force is then obtained from $F(b) = -dW/d(2b)$.

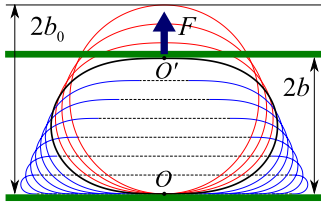


Fig. 1. (Color online) A thin-walled elastic tube deformed between two parallel plates. The thick black contour line marks the profile at the critical value $b_c/b_0=0.717770\dots$. The thinner lines above and below correspond to values of b/b_0 between 0 and 1.

III. ANALYTIC SOLUTION

A. Lagrangian formulation and analogy to the pendulum

An intrinsic quantity characterizing the shape of a planar curve is its tangential angle $\theta(s)$ defined as $\{\dot{x}, \dot{y}\} = \{\cos \theta, \sin \theta\}$. (A dot denotes the derivative with respect to s .) A particular advantage of employing $\theta(s)$ is that the (signed) curvature becomes $K = \dot{\theta}$.³ Integrating $\dot{x} = \cos \theta$ over the right half of the profile between the contact points O and O' gives the expression for the constraint (2) in integral form,

$$\int_0^{\pi b_0} \cos \theta(s) ds = 2b = \frac{2b}{\pi b_0} \int_0^{\pi b_0} ds. \quad (3)$$

At the points of contact between the foil and the plates, the tangent to the profile must be parallel to the y -axis. Hence, the boundary conditions for $\theta(s)$ are

$$\theta(s=0) = -\pi/2, \quad \theta(s=\pi b_0) = +\pi/2. \quad (4)$$

A standard way of converting a constrained optimization problem to an unconstrained one is the use of Lagrange multipliers. In our problem, both the target function W and the constraint (3) are expressed as integrals (functionals) of the unknown function $\theta(s)$. We denote the Lagrange multiplier for Eq. (3) by ω_0^2 (for reasons that will become clear) and use left-right symmetry in Eq. (1) to show that the variational problem becomes that of unconstrained minimization with respect to $\theta(s)$ and the quantity ω_0^2 of the functional

$$\tilde{W} = \frac{1}{2} \frac{W}{\kappa h} = \int_0^{\pi b_0} \mathcal{L}[\theta(s), \dot{\theta}(s), \omega_0^2] ds, \quad (5)$$

where

$$\mathcal{L} = \frac{1}{2} \dot{\theta}^2 + \omega_0^2 \cos \theta - \omega_0^2 \frac{2b}{\pi b_0}. \quad (6)$$

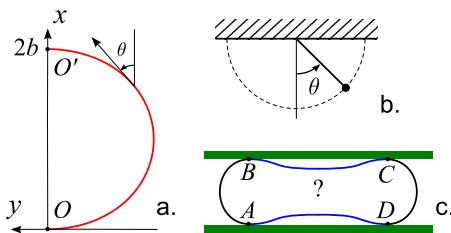


Fig. 2. (Color online) (a) Coordinate system for the profile energy calculation. (b) Equivalent pendulum problem with 90° maximal deviation. (c) A possible four-contact-point profile.

The analogy to the pendulum problem is now clear. If we interpret \tilde{W} as a dynamical action and s as a time, we recognize in Eq. (6) the Lagrange function of a rigid pendulum in a uniform gravitational field with the angular frequency of small oscillations equal to ω_0 [see Fig. 2(b)]. In the pendulum problem, θ is the angle of deviation from stable equilibrium and satisfies Newton's equation (the Euler-Lagrange equation of the variational problem),⁵

$$\ddot{\theta} + \omega_0^2 \sin \theta = 0. \quad (7)$$

In a standard mechanics problem ω_0 is usually given, and the boundary conditions (4) are satisfied by choosing the appropriate initial velocity $\dot{\theta}(0) \equiv K_0$, which depends on ω_0 . In our case, both ω_0 and K_0 are not known *a priori* and must be determined by satisfying the boundary conditions (4) and the constraint (3). The optimal value of ω_0^2 is proportional to the elastic force, because after integrating out the pendulum degree of freedom [that is, substituting $\theta(s)$ into the Lagrange function with the actual solution to the equation of motion (7)], $\tilde{W}(\omega_0, b)$ satisfies $\partial \tilde{W} / \partial \omega_0 = 0$, and thus

$$F = -\kappa h \frac{d\tilde{W}(\omega_0, b)}{db} = -\kappa h \frac{\partial \tilde{W}}{\partial b} = 2\kappa h \omega_0^2. \quad (8)$$

We shall use this property of Lagrange multipliers to calculate $F(b)$.

Before tackling the mostly mathematical problem of finding K_0 and ω_0 , we give arguments for the power-law dependence, which constitutes our most important result.

B. Power-law dependence, $b \leq b_c$

Qualitatively, $K_0(b)$ starts from $K_0(b_0) = 1/b_0$ and decreases as b is decreased. At the critical value $b = b_c$ (in the sense of separating two qualitatively different behaviors), the contact curvature vanishes, $K_0(b_c) = 0$. The corresponding pendulum problem becomes that of free oscillations with amplitude $\pi/2$ and frequency $\omega_0(b_c) = \omega_c$. The period of these oscillations is $T_0 = 4K(1/2)/\omega_c$,⁶ where K is the complete elliptic integral of the first kind. [This result is derived in the following as a special case of Eq. (16).] According to Eq. (4), the period must be equal to $T_0 = 2\pi b_0$, and we obtain

$$\omega_c = \frac{1}{\zeta_0 b_0} \quad \text{with} \quad \zeta_0 \equiv \frac{\Gamma^2(3/4)}{\sqrt{\pi}} = 0.847213\dots \quad (9)$$

If b is decreased further below b_c , an extra condition not accounted for by the Lagrangian formulation (6) becomes relevant: the plates do not allow the foil to bend outward, and thus K_0 also remains zero for $b < b_c$. To accommodate the imposed small values of b without violating the rigid plates, a finite part of the foil in the vicinity of $s=0$ and $s=\pi b_0$ must remain flat, so that $K(s) = 0$. (These parts are marked by horizontal dashed lines in the profiles shown in Fig. 1.) Concurrently, the sections of the profile that do bend satisfy Eq. (7), although with $\omega_0(b) > \omega_c$. If we assume continuity in $K(s)$, we conclude that the deformed part of the profile for $b < b_c$ must start with $K_0 = 0$ (same as for $b = b_c$), but cover a length shorter than the full length $2\pi b_0$ of the foil cross-section. This shortening of the deformed part can only be accommodated by a faster pendulum because the frequency $\omega_0(b)$ of the latter remains the only adjustable (that

is, b -dependent) parameter for $b < b_c$. (The other parameter, K_0 , is pinned to zero by the presence of a finite flat part.) According to Eq. (7), changing ω_0 results in a uniform rescaling of the arc length parameter s , and therefore the bent parts of the profile for $b < b_c$ (marked by curved lines between the plates in Fig. 1) must be geometrically similar to the corresponding halves of the critical profile at $b = b_c$ (marked with a thick contour in Fig. 1).

Having established that the critical profile shape is universal (in the sense of being applicable for any value of b less than b_c), we can determine the power-law dependence of the force using simple dimensional considerations. The scaling of b and b_0 with b/b_0 fixed does not change the overall shape of the profile—the tangential angle θ remains the same function of s/b_0 . Therefore, the elastic energy (1) can be written as $W(b) = \kappa h U(b/b_0)/b_0$, where U is a dimensionless function of b/b_0 . For $b < b_c$ the flat parts of the profile do not contribute to the energy. The curved parts are similar to the critical profile but b/b_c times smaller. Thus, their energy must have a fixed $U(b/b_0) \rightarrow U(b_c/b_0)$ and rescaled $b_0 \rightarrow b_0 b/b_c$. This argument gives scaling for the energy $W \propto b^{-1}$, and, consequently, the force $F \propto b^{-2}$ for $b < b_c$. The prefactor is given by

$$F(b) = F_c \frac{b_c^2}{b^2} = 2\kappa h \frac{(b_c/b_0)^2}{\zeta_0^2} b^{-2} \quad (b < b_c), \quad (10)$$

where $F_c \equiv F(b = b_c)$ and Eqs. (8) and (9) have been used. The phenomenological “stadium profile” model, considered as a variational *ansatz* in Ref. 1, assumes a circle as the universal profile and predicts $F(b) = (\pi/2)\kappa h/b^2$, similar to Eq. (10). However, the critical shape is more efficient than a circle in minimizing the bending energy.

We can calculate the numerical prefactor in Eq. (10) exactly by determining b_c . To this end, we proceed to the integration of the pendulum’s equation of motion.

The first integral of Newton’s equation is the energy conservation law, $\dot{\theta}^2/2 - \omega_0^2 \cos \theta = \text{const}$. We take into account that $\cos \theta(s=0) = 0$ and find

$$\frac{1}{2} \dot{\theta}^2 = \frac{1}{2} K_0^2 + \omega_0^2 \cos \theta. \quad (11)$$

Integrating both sides of Eq. (11) with respect to s and θ , and then using Eq. (3) gives

$$\tilde{W} = \frac{1}{2} \int_0^{\pi b_0} \dot{\theta}^2 ds = \frac{\pi b_0 K_0^2}{2} + 2\omega_0^2 b, \quad (12)$$

$$= \frac{1}{2} \int_{-\pi/2}^{+\pi/2} \dot{\theta} d\theta = \omega_0 I_0(K_0/\omega_0), \quad (13)$$

where

$$I_n(\alpha) \equiv \frac{1}{2} \int_{-\pi/2}^{+\pi/2} (\alpha^2 + 2 \cos \theta)^{1/2-n} d\theta. \quad (14)$$

We can determine b_c from Eqs. (12) and (13). We substitute b_c , ω_c , and 0 for b , ω_0 , and K_0 , respectively, use the identity $\zeta_0 = I_0(0)/2$, and obtain

$$b_c = I_0(0)/(2\omega_c) = \zeta_0^2 b_0 \approx 0.71777 b_0. \quad (15)$$

The results (10) and (15) confirm Eq. (17) of Ref. 1 (with the numerical factor 0.912 corrected to $4\zeta_0^2/\pi \approx 0.91389$).

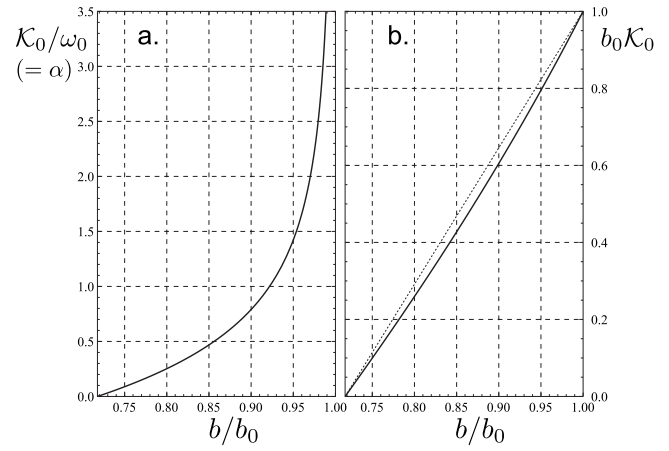


Fig. 3. (a) Graphical solution of Eq. (17). (b) The curvature at the contact point K_0 as a function of b/b_0 . The dashed line $(b-b_c)/(b_0-b_c)$ is plotted for visual guidance.

C. Small deformations, $b_0 > b > b_c$

For $b_0 > b > b_c$, $K_0 > 0$ and the relation between the period and the boundary conditions becomes more complicated. If we express $\omega_0 ds$ via $d\theta$ from Eq. (11) and integrate from $s = 0$ to $s = \pi b_0$, we obtain the required additional relation,

$$\pi b_0 \omega_0 = 2I_1(K_0/\omega_0). \quad (16)$$

Equation (16) yields the force after using Eq. (8). The remaining unknown is the parameter $\alpha \equiv K_0/\omega_0$, for which a single transcendental equation is obtained by combining Eqs. (12), (13), and (16),

$$\frac{b}{b_0} = \frac{\pi}{4} \left(\frac{I_0(\alpha)}{I_1(\alpha)} - \alpha^2 \right). \quad (17)$$

The function I_n in Eqs. (13), (16), and (17) can be reduced to standard elliptic integrals,⁷ $I_0(\alpha) = (4/k)\mathcal{E}(\pi/4, k^2)$ and $I_1(\alpha) = k\mathcal{F}(\pi/4, k^2)$, where \mathcal{E} and \mathcal{F} are incomplete elliptic integrals of the first and the second kind, respectively, and $k \equiv 2/\sqrt{2+\alpha^2}$ is the elliptic modulus. $I_1(0) = K(1/2) = \pi/(2\zeta_0)$, which is consistent with Eq. (9). We are unable to solve the transcendental equation (17) analytically and show the graphical solution in Fig. 3(a).

As b/b_0 changes from b_c/b_0 to 1, the only root of Eq. (17) goes from 0 to ∞ . The divergence of $\alpha = K_0/\omega_0$ as $b \rightarrow b_0$ is consistent with $\omega_0^2 \propto F \rightarrow 0$. The curvature at the contact point $K_0 = \alpha\omega_0$ is plotted in Fig. 3(b). K_0 decreases from $1/b_0$ to 0 as b goes from b_0 to b_c , in accordance with our previous discussion.

In summary, the exact solution for the elastic energy and the force for $b > b_c$ are

$$W = \frac{4\kappa h}{\pi b_0} I_0(\alpha) I_1(\alpha), \quad (18)$$

$$F = \frac{2\kappa h}{b_0^2} \left(\frac{2I_1(\alpha)}{\pi} \right)^2, \quad (19)$$

where $\alpha(b/b_0)$ is the root of Eq. (17), see Fig. 3(a).

D. Stability of the universal solution and bending-induced tension

After formulating an explicit solution for $b > b_c$, Eq. (18), we can justify the power-law dependence for $b < b_c$ more rigorously. It has been suggested¹ that for $b \leq 0.3b_0$, profiles with a slight curvature in the horizontal part may provide a better solution than a “stadium” with completely flat segments. Such a four-contact-point solution is sketched in Fig. 2(c) (the concave segments BC and AD are exaggerated). However, the following argument shows that any four-contact-point profile will have a larger bending energy than the optimal profile with straight segments BC and AD .

Let us fix the positions of the contact points on the profile by gluing the foil to the plates at A , B , C , and D . The curvature K_A must be the same at all of these four points due to symmetry, and furthermore, K_A is positive. Thus, the strongly curved parts AB and CD must conform to our solution for $K_0 = K_A > 0$ with a smaller b_0 adjusted to their respective shorter lengths. Now consider slightly increasing the lengths of AB and CD while making BC and AD shorter, so that the total circumference of the profile remains the same. In this new configuration, the energy of the segments BC and AD will be reduced. However, the corresponding lengthening of the segments AB and CD will also reduce their energy. For fixed b , longer (higher b_0) two-point profiles have lower minimum total energy, as can be shown explicitly using Eqs. (8), (16), (18), and (19),

$$F_T \equiv \left. \frac{dW}{d(2\pi b_0)} \right|_{b=\text{const}} = -\frac{\kappa h}{2} K_0^2 \leq 0. \quad (20)$$

Thus, we can always lower the bending energy of a four-point profile such as the one shown in Fig. 2(c), so that BC and AD become completely flat and can no longer be shortened. This minimal energy limit is the zero-contact-curvature universal stadium profile.

By definition, F_T/h is the surface tension energy of the deformed foil. Uniform tension may be induced in a cylindrically deformed foil by bending even if the stretching deformation is negligible.² The value from Eq. (20) for F_T and its independence of s can be confirmed using local Lagrange multipliers,⁸ which take the local tension into account explicitly.

If we recall that the foil is assumed to be made of uniform elastic material with bulk Young modulus E , we can estimate the neglected stretching deformation. Bending-induced negative surface tension is balanced by uniform linear stretching. By using Hooke’s law, we can express the increment in the profile circumference $2\pi\Delta b_0$ due to stretching as $\Delta b_0 = b_0 F_T / (Edh)$. The corresponding contribution of stretching $\Delta W_{\text{stretch}} \sim Ehd^5/b_0^3$ to the total energy $W \sim Ehd^3/b_0$ is negligible if $d^2 \ll b_0^2$, thus confirming our approximation of an unstretchable foil. The universal profile is tension free, $F_T(b \leq b_c) = 0$.

E. Critical shape

Before discussing our final results for the force, Eqs. (10) and (19), we briefly comment on the shape of the critical profile. If we use the explicit solution of the pendulum problem [obtained, for example, by integrating Eq. (11), see Ref. 6], and use several properties of the elliptic functions,⁷ we

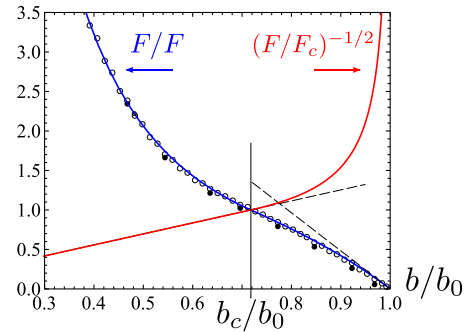


Fig. 4. (Color online) Elastic force F as a function of the half-height b , scaled by the critical force F_c and the undeformed cylinder radius b_0 , in linear and inverse square root representations. Circles: experimental data scaled by a single fitting parameter F_c . The spring was first gradually loaded (○) up to $b_{\min} = 0.4b_0$, and then unloaded (●).

can show that the shape of the profile at $b = b_c$, in units corresponding to $b_0 = 1/(\zeta_0\sqrt{2})$, is given parametrically for $\theta \in [-\pi/2, \pi/2]$ by

$$x(\theta) = \zeta_0/\sqrt{2} + \mathcal{E}(\theta/2, \sqrt{2}), \quad (21)$$

$$y(\theta) = \pm \sqrt{\cos \theta}, \quad (22)$$

with the arc length $s(\theta) = \pi b_0/2 + \mathcal{F}(\theta/2, \sqrt{2})$. This shape is shown in Fig. 1 by the thick contour touching the plates. Profile shapes for $b > b_c$ are obtained by integrating Eq. (7) numerically with the initial condition obtained from Eqs. (16) and (17) and shown by thin lines reaching above the upper plate in Fig. 1.

IV. DISCUSSION AND COMPARISON TO EXPERIMENT

The final results for the force are shown in Fig. 4. We use $F_c = 2\kappa h/(\zeta_0 b_0)^2$ to express the force into the dimensionless form, $F(b)/F_c$, which is a single universal function of b/b_0 . This function is shown by continuous lines in Fig. 4; also plotted is $(F(b)/F_c)^{-1/2}$ to reveal the range of power-law dependence. The point $b = b_c$ is an inflection point of $F(b)$ (with a jump in the third derivative).

It is instructive to verify that the rolled foil behaves as a linear spring when close to a cylindrical shape (that is, as $b \rightarrow b_0$). If we use the definition of $I_n(\alpha)$ to obtain the large α expansion, we obtain α from Eq. (17), $b_0 - b \sim (\pi/4 - 2/\pi)\alpha^{-2}b_0$, and $F(b)$ from Eq. (19) as

$$F(b) = \frac{2\kappa h}{b_0^2} \frac{b_0 - b}{b_0} \frac{4\pi}{\pi^2 - 8}, \quad (b \rightarrow b_0). \quad (23)$$

This linear behavior is marked by a dashed line in the lower right corner of Fig. 4.

Measurements of $F(b)$ have been performed using the setup and one of the samples (blue plastic binding covers, set 1) described in Ref. 1. The results are shown in Fig. 4 by circles on a linear scale (see the logarithmic scale used in Ref. 1, Fig. 5). The spring was gradually loaded from $b = b_0$ down to $b_{\min} = 0.4b_0$ (open circles) and then unloaded by increasing b up to zero force (filled circles). Note the hysteresis due to inelastic deformations. The corresponding energy loss (hysteresis loop area) is 4% of $W(b_{\min})$. The critical force

$F_c=116$ N with relative error of 3% (estimated from the residuals between the open data points and the analytical fit) corresponds to a bending rigidity of $\kappa=(1.48 \pm 0.04)$ mJ, in reasonable agreement with Ref. 1.

ACKNOWLEDGMENTS

The author is thankful to Paul Stanley and Eli Raz for inspiring discussions of the problem.

^{a)}Electronic mail: slava@latnet.lv

¹A. Šiber and H. Buljan, "Theoretical and experimental analysis of a thin elastic cylindrical tube acting as a non-Hookean spring," arXiv:cond-mat/1007.4699v1.

²L. Landau and E. Lifshitz, *Theory of Elasticity*, 3rd ed. (Pergamon, London, 1986).

³D. J. Struik, *Lectures on Classical Differential Geometry*, 2nd ed. (Dover, New York, 1988).

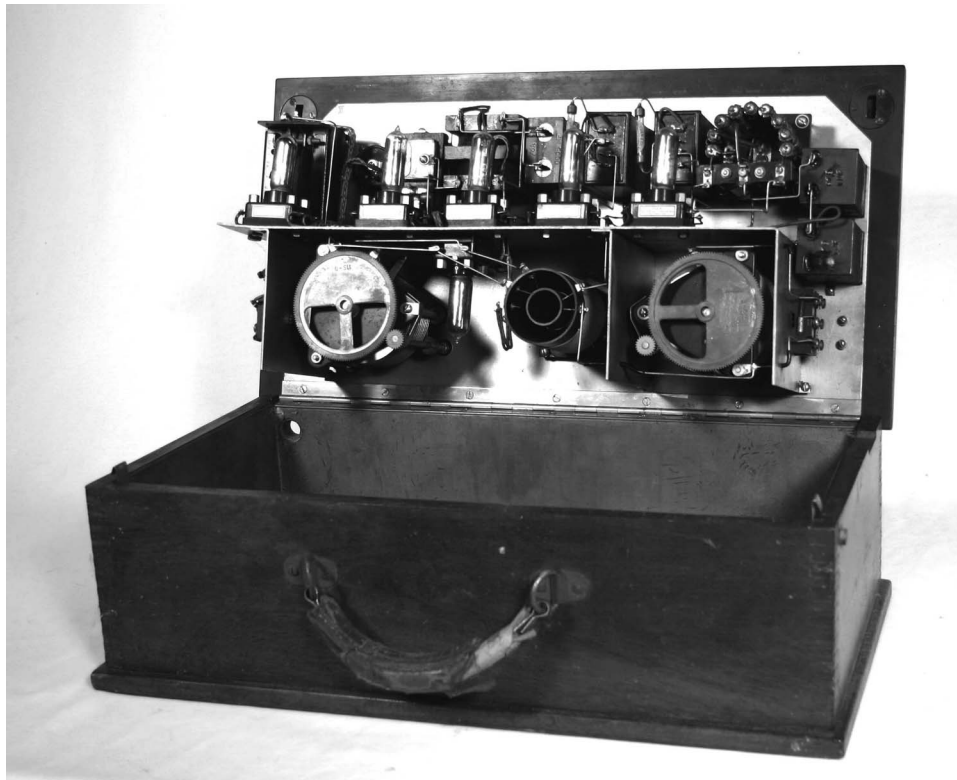
⁴The accuracy of the unstretchability assumption will be estimated *a posteriori*.

⁵For an alternative way to derive Eq. (7), see Ref. 2, Sec. 19, Problem 1.

⁶A. Beléndez, C. Pascual, D. I. Méndez, T. Beléndez, and C. Neipp, "Exact solution for the nonlinear pendulum," *Revista Brasileira de Ensino de Física* **29**, 645–648 (2007).

⁷M. Abramowitz and I. A. Stegun, *Handbook of Mathematical Functions with Formulas, Graphs, and Mathematical Tables*, 9th ed. (Dover, New York, 1972), pp. 567–581.

⁸A. Cēbers, "Dynamics of a chain of magnetic particles connected with elastic linkers," *J. Phys.: Condens. Matter* **15**, S1335–S1344 (2003).



Superhetrodyne radio receiver. This radio receiver was sold in 1925 at the time that the radio-listening public was passing out of the crystal set era. The Superhetrodyne technique was invented by the electrical engineer Edwin H. Armstrong and continues to be used in AM radios. The Western Electric peanut tubes are curiously small compared to those in use in subsequent years. The instrument was donated to the Greenslade Collection by Clarence Bennett. (Notes and photograph by Thomas B. Greenslade, Jr., Kenyon College)